University of Nebraska - Lincoln

DigitalCommons@University of Nebraska - Lincoln

2000

Two-step Processing of Human Frataxin by Mitochondrial Processing Peptidase

Patrizia Cavadini
Mayo Clinic and Foundation

Jiri Adamec
University of Nebraska-Lincoln, jadamec2@unl.edu

Franco Taroni
Istituto Nazionale Neurologico "Carlo Besta," Milano, Italy

Oleksandr Gakh
Academy of Sciences of the Czech Republic

Grazia Isaya
Mayo Clinic and Foundation

Follow this and additional works at: http://digitalcommons.unl.edu/biochemfacpub

Part of the Biochemistry Commons, Biotechnology Commons, and the Other Biochemistry, Biophysics, and Structural Biology Commons

Two-step Processing of Human Frataxin by Mitochondrial Processing Peptidase

PRECURSOR AND INTERMEDIATE FORMS ARE CLEAVED AT DIFFERENT RATES*

Patrizia Cavadini‡§¶, Jiri Adamec‡, Franco Taroni§‡‡, Oleksandr Gakh‖, and Grazia Isaya‡**

From the ‡Department of Pediatric & Adolescent Medicine and Biochemistry & Molecular Biology, Mayo Clinic and Foundation, 200 First Street SW, Rochester, Minnesota 55905, the §Division of Biochemistry and Genetics, Istituto Nazionale Neurologico "Carlo Besta," Milano, Italy, and the ‖Institute of Microbiology, Academy of Sciences of the Czech Republic, Prague, Czech Republic 14220

We showed previously that maturation of the human frataxin precursor (p-fxn) involves two cleavages by the mitochondrial processing peptidase (MPP). This observation was not confirmed by another group, however, who reported only one cleavage. Here, we demonstrate conclusively that MPP cleaves p-fxn in two sequential steps, yielding a 18,826-Da intermediate (i-fxn) and a 17,255-Da mature (m-fxn) form, the latter corresponding to endogenous frataxin in human tissues. The two cleavages occur between residues 41–42 and 55–56, and both match the MPP consensus sequence R$X \downarrow$ (*X*/S). Recombinant rat and yeast MPP catalyze the p $\rightarrow$ i step 4 and 40 times faster, respectively, than the i $\rightarrow$ m step. In isolated rat mitochondria, p-fxn undergoes a sequence of cleavages, p $\rightarrow$ i $\rightarrow$ m $\rightarrow$ d$_1$ $\rightarrow$ d$_2$, with d$_1$ and d$_2$ representing two C-terminal fragments of m-fxn produced by an unknown protease. The i $\rightarrow$ m step is limiting, and the overall rate of p $\rightarrow$ i $\rightarrow$ m does not exceed the rate of m $\rightarrow$ d$_1$ $\rightarrow$ d$_2$, such that the levels of m-fxn do not change during incubations as long as 3 h. Inhibition of the i $\rightarrow$ m step by a disease-causing frataxin mutation (W173G) leads to nonspecific degradation of i-fxn. Thus, the second of the two processing steps catalyzed by MPP limits the levels of mature frataxin within mitochondria.

Frataxin is a nucleus-encoded mitochondrial protein widely conserved among eukaryotes, believed to play a critical role in mitochondrial iron homeostasis (reviewed in Ref. 1). Disruption of the yeast frataxin gene (*YFH1*) leads to mitochondrial iron overload and loss of respiratory function (2, 3), whereas yeast frataxin (Yfh1p) was recently shown to bind iron and maintain it in an available form (4). In humans, frataxin deficiency leads to Friedreich ataxia (FRDA),[1] an autosomal recessive disease characterized by progressive neurodegeneration in the spinal cord and hypertrophic cardiomyopathy (5). Most FRDA patients are homozygous for GAA repeat expansions in the first intron of the frataxin gene (6) and show reduced levels of frataxin ranging from 6 to 30% of normal levels (7). 4% of FRDA patients have one GAA expansion and a truncating or missense mutation on the other allele and show either a typical FRDA phenotype or milder clinical presentations, depending on the point mutation (8). Even though frataxin is expressed in all tissues (6, 7), the pathology of FRDA is limited to certain regions of the central nervous system and heart (5), whereas biochemical evidence of abnormal mitochondrial iron homeostasis has been detected almost exclusively in heart (9). On the other hand, disruption of the mouse frataxin gene is incompatible with normal development and results in early embryonic lethality without apparent iron accumulation (10).

The spectrum of manifestations associated with frataxin defects indicates that a number of factors must influence the function of frataxin in different organisms and cell types. Several observations suggest that proteolytic processing of frataxin is likely to play an important role in influencing the levels of mature frataxin within mitochondria. Similar to most mitochondrial proteins, frataxin is initially synthesized in the cytoplasm as a larger precursor with a N-terminal presequence that targets frataxin to the mitochondrial matrix (2, 11, 12). In a yeast two-hybrid screen, Koutnikova *et al.* (13) found a direct interaction between the precursor form of mouse frataxin and the β subunit of the mitochondrial processing peptidase (MPP; EC 3.4.24.64). In processing assays using bacterially expressed MPP, they observed cleavage of the mouse frataxin precursor to a product with an apparent molecular mass of 21 kDa, larger than the apparent molecular mass of endogenous frataxin (∼18 kDa), as detected in mouse and human tissues at steady state (7, 13). We later showed that both a ∼21-kDa product and a ∼18-kDa product are obtained by cleavage of the human frataxin precursor by recombinant MPP (12). However, formation of the 18-kDa product was inefficient under our experimental conditions (12) and was not detected at all by another group, who reported that human frataxin is actually processed to the mature form in a single step (14). Unlike human and mouse frataxin, Yfh1p is efficiently cleaved to the mature form in two sequential steps, and purified MPP is necessary and sufficient to carry out both cleavages *in vitro* (12), whereas the mitochondrial Hsp70 homologue, Ssq1, is required for the second cleavage in isolated yeast mitochondria (11) and, to a lesser extent, in intact yeast cells (15).

Most nuclear-encoded mitochondrial precursors are processed to their mature form by MPP, and even though the length of the targeting signal may vary considerably among different proteins, only one cleavage is normally required (16). Two-step processing by MPP represents a rare variation that

[1] The abbreviations used are: FRDA, Friedreich ataxia; MPP, mitochondrial processing peptidase; fxn, human frataxin; p-fxn, precursor form of fxn; i-fxn, intermediate form of fxn; m-fxn, mature form of fxn; PCR, polymerase chain reaction; PAGE, polyacrylamide gel electrophoresis.

has thus far been observed only for the *Neurospora crassa* ATPase subunit 9 (17), yeast frataxin (11, 12, 15), and, in our hands, human frataxin (12). In this study, we present conclusive evidence that p-fxn is processed to the mature form in two sequential steps. We show that the precursor is cleaved rapidly and quantitatively to the intermediate form, whereas the i → m reaction is slower and limits the overall rate at which m-fxn is produced within mitochondria. This reaction is further inhibited by a known FRDA point mutation, suggesting that defects in i → m processing may contribute to the disease.

EXPERIMENTAL PROCEDURES

Constructs and Strains—The 5′-and 3′-untranslated regions of the FRDA cDNA were modified by PCR using primers 5′HUMYB-S (5′-cgcggatccgtagcaatgtggactctcgggcgc-3′), introducing a *Bam*HI site and the ribosome-binding site of the *YFH1* gene transcript immediately upstream of the initiator ATG, and 3′HUMB-AS (5′-cgcggatccctcaagcatcttttccggaata-3′), introducing a *Bam*HI site downstream of the stop codon, or 3′HUMMet-AS (5′-cgcggatcctcacatcatagcatcttttccggaata-3′), introducing two ATG upstream and a *Bam*HI site downstream of the stop codon. The two PCR products, FRDA and FRDAMet, were cloned in the *Bam*HI site of a *TRP1*-based, 2-μm yeast expression vector, pG-3 (18), downstream of the yeast glyceraldehyde-3-phosphate dehydrogenase promoter, yielding plasmids pG3-FRDA and pG3-FRDAMet.

For *in vitro* expression, the FRDAMet PCR product was cloned into the *Bam*HI site of vector pGEM-3Zf(+) (Promega), yielding plasmid pGEM-FRDAMet. To obtain molecular mass markers to map the i-fxn and m-fxn N termini, the 5′ region of the FRDA cDNA was deleted by use of two forward primers including a *Bam*HI site, a Kozak sequence, an ATG codon, and codons 43–49 (5′-gcggatccgccaccatgcgcaccgacatcgatgcgacc-3′) or 57–63 (5′-cgcggatccgccaccatgtcgaaccaacgtggcctcaac-3′) of the FRDA cDNA, coupled with primer 3′HUMMet-AS, yielding constructs pGEM-FRDA(L42M) and pGEM-FRDA(S56M). For analysis of FRDA point mutations, forward primers encoding the desired point mutations were coupled with the 3′HUMMet-AS primer, and the resulting PCR products used as antisense primers were coupled with the 5′HUMYB-S primer. The final PCR products were digested with *Not*I and *Bsp*EI, and the 505-base pair fragment was subcloned into plasmid YC-FRDA, yielding YC-FRDA(G130V) and YC-FRDA(W173G) vectors (19). A 647-base pair *Bam*HI fragment was excised from these vectors and cloned into pGEM-3Zf(+), yielding constructs pGEM-G130V and pGEM-W173G (19).

For radiosequencing, the FRDA cDNA was modified using primers 5′KMetB-S (5′-cgcggatccgccaccatgtggactctcctcgggcgc-3′) including a *Bam*HI site, a Kozak sequence, and the 5′-end of the FRDA coding sequence, and Leu62Met-AS (5′-attccaaatctggttcatgccacgttggttcga-3′), including codons 57–67 of FRDA, with a CTC → ATG change at codon 62. This PCR product was coupled with primer 3′HUMB-AS, and the final PCR product was cloned into pGEM-3Zf(+), yielding plasmid pGEM-FRDA(L62M). For radiosequencing of i-fxn-G130V and i-fxn-W173G, the G130V or W173G mutation was introduced in the pGEM-FRDA(L62M) construct to yield the pGEM-FRDA(L62M/G130V) or pGEM-FRDA(L62M/W173G) construct. All constructs were verified by DNA sequencing.

The *yfh1*Δ and complemented *yfh1*Δ[*YFH1*] strains were described previously (20). To produce a fxn-expressing strain, *yfh1*Δ[*YFH1*] was transformed with plasmid pG3-FRDA and pG3-FRDAMet, and the *URA3*-based YCp50-YFH1 plasmid was eliminated by counterselection with 5-fluoroorotic acid (21), yielding the *yfh1*Δ[pG3-FRDA] and *yfh1*Δ[pG3-FRDAMet] strains.

Western Blotting—Yeast cells were grown in 5 ml of YPD (2% peptone, 1% yeast extract, 2% dextrose) to late log phase at 30 °C, and total extracts were prepared as described (20). Frozen human tissue samples (kindly provided by A. W. Strauss, Washington University, St. Louis, MO, and P. Rinaldo, Mayo Clinic, Rochester, NY) were homogenized in 10 mM Tris-HCl, pH 7.4, 10 mM EDTA, 150 mM NaCl, and centrifuged at 800 × *g* for 10′. The supernatant was incubated with 0.25% SDS, 2% Triton X-100, 1000 units/ml aprotinin, 20 μg/ml leupeptin, 2 μg/ml pepstatin, and 1 mM phenylmethylsulfonyl fluoride, for 1 h at 4 °C, and clarified by centrifugation at 100,000 × *g* for 30′. Protein concentration was determined by the BCA™ protein assay kit (Pierce). Anti-Yfh1p antibodies were as previously described (19, 20).

Mitochondrial Import and Processing Assays and N-terminal Radiosequencing—All constructs used in this study were synthesized *in vitro* in the presence of [35S]methionine using TNT Quick coupled transcription/translation system (Promega). Previously described procedures

were used for mitochondrial import and processing assays (12) and for expression and purification of yeast and rat MPP (22).[2] Processing and import reactions were analyzed by SDS/PAGE using *T* = 12.5% separating gels (where *T* denotes the total concentration of acrylamide and bisacrylamide), from a stock solution of acrylamide:bisacrylamide = 40:1.7. Electrophoresis was started at 160 V, shifted to 230 V after the samples had completely entered the separating gel, and continued for an additional 45 min after the samples had reached the bottom of the gel. For N-terminal radiosequencing, the pGEM-FRDA(L62M), pGEM-FRDA(L62M/G130V), and pGEM-FRDA(L62M/W173G) constructs were transcribed and translated *in vitro* in the presence of [35S]methionine, and radiolabeled precursors were incubated with recombinant yeast MPP. Processing products were separated by SDS/PAGE, electroblotted onto a polyvinylidene difluoride membrane (Millipore), and detected by autoradiography. The desired band was excised and applied directly on a PE/ABD Procise 494-HS sequencer, and 100% of each fraction was collected and analyzed by scintillation counting (24).

RESULTS

Identification of the i-fxn and m-fxn N Termini—We and others showed previously that p-fxn is processed by MPP to two smaller products with apparent molecular mass on SDS/PAGE of 21,000 (i-fxn) and 18,000 Da (m-fxn) (12, 13). The 21-kDa product was shown to co-migrate with a polypeptide corresponding to residues 41–210 of p-fxn (13), and the 18-kDa product was shown to co-migrate with endogenous frataxin in human tissues (12, 13). In a more recent study of p-fxn processing, however, Gordon *et al.* (14) detected only the 21-kDa product and concluded that this represents the mature form of fxn. To clarify this apparent discrepancy, we re-examined the processing of p-fxn by recombinant yeast MPP. To enhance detection of 35S-labeled m-fxn by SDS/PAGE and fluorography, a two-methionine tag was fused in frame to the C terminus of p-fxn. Processing of this construct yielded two products, i-fxn and m-fxn, that co-migrated with standard polypeptides corresponding to residues 42–210 and 56–210, respectively, of p-fxn (Fig. 1*A*). Whereas p-fxn was efficiently converted to i-fxn, processing of i-fxn to m-fxn was significantly less efficient (Fig. 1*A*), and if we used a precursor lacking the two-methionine tag, we detected only trace amounts of m-fxn (not shown). This suggests that Gordon *et al.* (14) may have not identified the 18-kDa product because their method for detection was not sufficiently sensitive. N-terminal radiosequencing of i-fxn and m-fxn revealed that the former is processed between residues 41 and 42 (RRG ↓ LRT) (Fig. 1*B*), and the latter is processed between residues 55 and 56 (RRA ↓ SSN) (Fig. 1*C*), with both cleavages matching the MPP consensus sequence R*X* ↓ (*X*/S) (25). Lack of detectability may explain why Gordon *et al.* (14) identified the peptide predicted to be released by the first cleavage (residues 1–41, ~4 kDa) but not the much shorter peptide predicted to be released by the second cleavage (residues 42–55, ~1.4 kDa). The calculated molecular masses of the intermediate and mature form of frataxin are 18,826 and 17,255 Da, slightly lower than predicted from their mobility on SDS/PAGE. Similarly, p-fxn has a calculated molecular mass of 23,135 Da, lower than its apparent molecular mass of 30,000 Da on SDS/PAGE (Fig. 1*A*). Abnormal mobility on SDS/PAGE has also been reported for the Yfh1p precursor and its processing products (11, 12), and is explained by the acidic nature of these proteins.

m-fxn Corresponds to Endogenous Frataxin in Human Tissues—To exclude the possibility that the two-methionine tag might somehow alter the processing of p-fxn, precursor polypeptides with or without the tag were expressed in yeast and analyzed by Western blotting (Fig. 2*A* and not shown). We have recently shown that a full-length human frataxin precur-
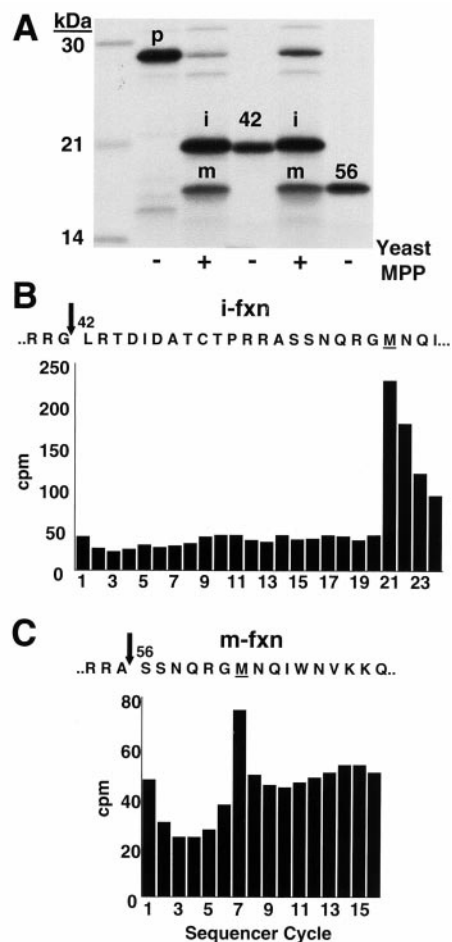
FIG. 1. **Determination of the i-fxn and m-fxn processing sites.** *A*, radiolabeled p-fxn was synthesized by coupled *in vitro* transcription-translation in the presence of [35S]methionine and incubated with purified yeast MPP. Processing reactions were analyzed by SDS/PAGE and fluorography. The letters *p*, *i*, and *m* denote the precursor, intermediate, and mature forms of fxn; *42* and *56* denote N-terminally truncated polypeptides translated from methionine residues replacing Leu[42] and Ser[56] in the p-fxn sequence. *B* and *C*, N-terminal radiosequencing of i-fxn and m-fxn. A methionine residue (*underlined*) was substituted for leucine 62 to provide a radioactive marker downstream of the predicted m-fxn N terminus (*i.e.* Ser[56]). [35S]Methionine-labeled p-fxn(L62M) was incubated with yeast MPP, and the processing products were separated by SDS/PAGE, electroblotted, and detected by autoradiography. The i-fxn and m-fxn bands were excised and subjected to N-terminal sequencing, and 100% of each fraction was analyzed by scintillation counting. *B*, Leu[42] marks the N terminus of i-fxn as determined by release of [35S]methionine in cycle 21. *C*, Ser[56] marks the N terminus of m-fxn as determined by release of [35S]methionine in cycle 7. Because of inefficient processing of i-fxn to m-fxn, the m-fxn sample contained a small amount of protein and the level of isotope released in cycle 7 was only slightly above background.

sor complements yeast cells lacking endogenous Yfh1p (19). Accordingly, both *yfh1*Δ[pG3-FRDA] and *yfh1*Δ[pG3-FR-DAMet] cells exhibited a normal phenotype (not shown). Total extracts from *yfh1*Δ[pG3-FRDA] cells contained two products of 21 and 18 kDa (*lane 2*) that were not detected in *yfh1*Δ[*YFH1*] (*lane 1*). Two slightly larger products were detected in *yfh1*Δ[pG3-FRDAMet] cells and found to co-migrate with the i-fxn and m-fxn products obtained by *in vitro* processing of p-fxn (not shown). These products associated with the mitochondrial fraction (*lane 4*) and were protected from externally added proteinase K (*lane 3*). The 18-kDa product detected in *yfh1*Δ[pG3-FRDA] cells co-migrated with a bacterially expressed protein translated from a methionine residue replacing serine 56 (*i.e.* the N terminus of m-fxn, as determined by
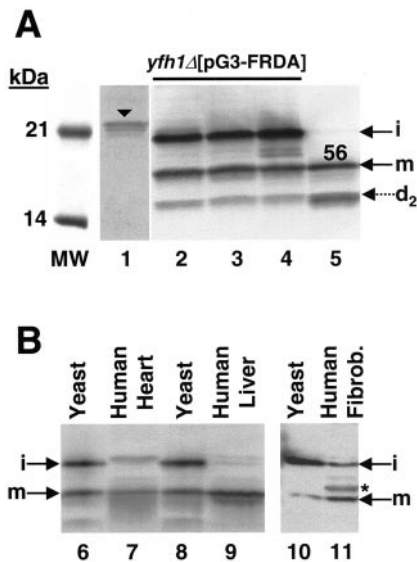

FIG. 2. **m-fxn corresponds to endogenous frataxin in human tissues.** *A*, total cell extracts from strain *yfh1*Δ[*YFH1*] (*lane 1*) and *yfh1*Δ[pG3-FRDA] (*lane 2*) (100 µg of total protein/lane) and isolated mitochondria from *yfh1*Δ[pG3-FRDA] with (*lane 3*) and without (*lane 4*) proteinase K treatment (40 µg of total protein/lane) were analyzed by Western blotting using anti-fxn antibody. The *arrowhead* indicates the mature form of Yfh1p (*lane 1*), that is recognized by the anti-fxn antibody; *56* denotes a bacterially expressed polypeptide translated from a methionine that replaces serine 56 (*lane 5*, 2 ng of total protein), and *d2* denotes a degradation product. *MW*, molecular weight markers. *B*, total extracts from *yfh1*Δ[pG3-FRDA] yeast (*lanes 6*, *8*, and *10*; 30 µg of total protein/lane), human heart, liver, and fibroblasts (*lanes 7*, *9*, and *11*, respectively; 100 µg total protein/lane) were analyzed by Western blotting as described above. The band marked by an *asterisk* was only detected in fibroblasts and may represent a nonspecific cross-reacting product.

radiosequencing in Fig. 1*C*, *lane 5*). The 18-kDa product was also found to co-migrate with endogenous frataxin in three different human tissues (Fig. 2*B*, *lanes 7*, *9*, and *11*).

MPP Cleaves p-fxn and i-fxn at Different Rates in Vitro—Unlike m-fxn, the intermediate form was not consistently seen in human tissues. For example, i-fxn was not detected in heart (Fig. 2*B*, *lane 7*) but was present in trace amounts in liver (*lane 9*) and in more discrete amounts in fibroblasts (*lane 11*). This suggests that a kinetic effect may be responsible for the accumulation of i-fxn in Fig. 1*A*. To determine the rates of p → i and i → m processing, radiolabeled p-fxn was incubated with an excess of yeast MPP, and aliquots were analyzed at different time points. Whereas most input p-fxn was converted to i-fxn within the first 5′ of incubation, less than 20% of i-fxn was converted to m-fxn after an additional 25′ (Fig. 3*A*). Determination of the initial rates of the p → i and i → m reactions showed that the first reaction is 40 times faster than the second (Fig. 3*B*). Under similar experimental conditions, the yeast frataxin precursor was rapidly and quantitatively processed to the mature form in two steps (not shown), raising the possibility that species specificity may be important for the i → m reaction. Indeed, recombinant rat MPP cleaved p-fxn more efficiently as compared with yeast MPP (Fig. 4*A*). The input p-fxn was almost completely processed to i-fxn in 5′, and i-fxn was quantitatively converted to the mature form after an additional 25′. Nevertheless, the initial rate of the p → i reaction was 12 times faster than that of the i → m reaction (Fig. 4*B*).
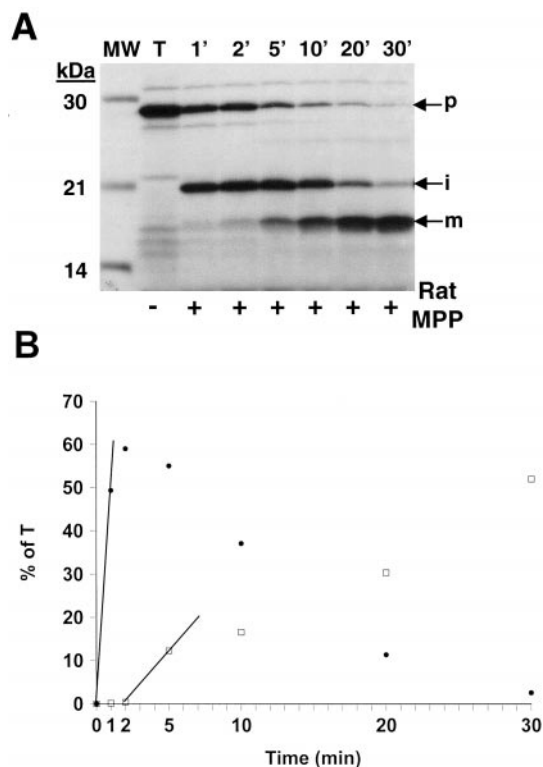
p-fxn and i-fxn Are Processed at Different Rates in Isolated Rat Mitochondria—Previous studies have shown that processing of the intermediate form of Yfh1p is impaired in yeast cells with defects in the mitochondrial Hsp70 homologue, Ssq1 (11, 15). This suggests that a human homologue of Ssq1 or some

Two-step Processing of Human Frataxin
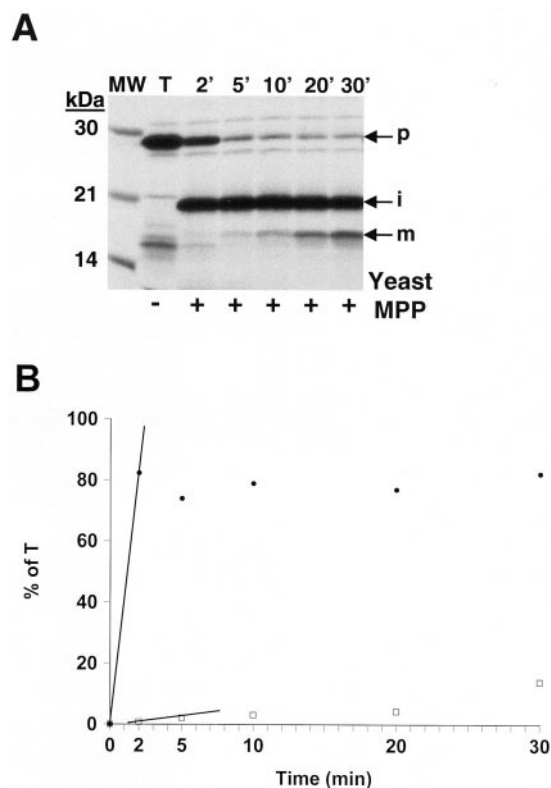
FIG. 3. **Two-step processing of p-fxn and pYfh1p by recombinant yeast MPP.** *A*, radiolabeled precursor was incubated with an excess of recombinant yeast MPP (final enzyme concentration, 600 ng/μl), and aliquots of the processing reaction were analyzed by SDS/PAGE at the indicated time points. *T*, control reactions incubated for 30 min without MPP. *B*, the levels of i (*filled circles*) and m (*open squares*) at each time point were determined by densitometry, expressed as percentages of the input precursor (*T*), and plotted *versus* time. The initial rate (V_0) of p $\rightarrow$ i and i $\rightarrow$ m was deduced from the two linear fit lines. The Δi/Δt slope corresponds to $V_0 = 41$, and the Δm/Δt slope corresponds to $V_0 = 0.5$.

FIG. 4. **Two-step processing of p-fxn by recombinant rat MPP.** *A*, radiolabeled p-fxn was incubated with an excess of recombinant rat MPP (final enzyme concentration, 400 ng/μl) and aliquots of the processing reaction analyzed as in Fig. 3*A*. *T*, control reaction incubated for 30 min without MPP. *B*, the levels of i (*filled circles*) and m (*open squares*) were determined, and the V_0 of p $\rightarrow$ i and i $\rightarrow$ m deduced from the two linear fit lines as in the legend of Fig. 3*B*. The Δi/Δt slope corresponds to $V_0 = 49$, and the Δm/Δt slope corresponds to $V_0 = 4$.

other mitochondrial protein may be required for the maturation of human frataxin. In such a case, two-step processing of p-fxn should be more efficient upon import into intact mitochondria, that contain MPP and presumably all other factors involved in the maturation of frataxin *in vivo*. This prediction was not confirmed experimentally, however. Whereas >50% of the input p-fxn was rapidly imported and processed to i-fxn by isolated rat liver mitochondria (Fig. 5*A*, *lane 3*), <20% of this i-fxn was converted to the mature form after 60′ of incubation (*lane 6*). Because i-fxn was protected from externally added proteinase K (*lane 7*), lack of i-fxn processing did not result from incomplete translocation of i-fxn. Given that human frataxin is highly expressed in heart and significantly less in liver (6), we tested the possibility that processing of i-fxn might be more efficient in rat heart mitochondria, but we observed a rate of i $\rightarrow$ m conversion as slow as with rat liver mitochondria (not shown). The i-fxn processing efficiency was not improved by adding an ATP-regenerating system to the import reaction or using different incubation temperatures (4, 16, or 37 °C) (not shown).

i-fxn Is Chased into Smaller Degradation Products in Isolated Mitochondria—Under the conditions tested above, p-fxn was converted to i-fxn in excess of the rate at which i-fxn could be processed to m-fxn, leading to i-fxn accumulation. In human tissues, however, i-fxn is either undetectable or significantly less abundant than the mature form (Fig. 2*B*). To analyze the turnover rates of i-fxn and m-fxn, radiolabeled p-fxn was incubated with rat liver mitochondria for 30′ at 27 °C, proteinase K

was added to digest any precursor that had not been imported, and the incubation continued for another 3 h at 27 °C. During the chase, we observed a progressive reduction in the i-fxn levels (Fig. 5*B*) with concomitant appearance of two smaller products (d$_1$ and d$_2$) and essentially unchanged levels of m-fxn. In a similar experiment, the turnover rates of i-fxn and m-fxn were analyzed and compared at 27 and 37 °C. Whereas i-fxn levels decreased more rapidly at 37 °C, m-fxn levels remained essentially unchanged at both temperatures (Fig. 5*C*). These data suggest that i-fxn is slowly processed by MPP to m-fxn, which is steadily degraded to smaller products. Another possible interpretation is that only a fraction of i-fxn is processed to m-fxn, whereas most intermediate is degraded to smaller products. In either case, limited processing of i-fxn by MPP, coupled with rapid degradation of i-fxn and/or m-fxn by an as yet unknown protease, appear to influence the levels of m-fxn in isolated mitochondria.

The G130V FRDA Point Mutation Does Not Affect Processing of p-fxn by MPP—Koutnikova *et al.* (13) reported previously that the two most frequent FRDA point mutations, I154F and G130V (8), reduce binding of p-fxn to MPP as determined by use of a yeast two-hybrid system, suggesting that even mutations far from the MPP cleavage sites may affect processing. These authors showed that the I154F mutation affects the p $\rightarrow$ i step in COS cells, but Gordon *et al.* (14) later showed that this step occurs normally when the mutant precursor is processed by recombinant MPP or isolated mitochondria. We analyzed the G130V mutation and found that it was associated with rates of p $\rightarrow$ i and i $\rightarrow$ m processing (Fig. 6) comparable with those of wild type p-fxn (Fig. 3*A*). The processing products derived from p-fxn-G130V exhibited a lower electrophoretic
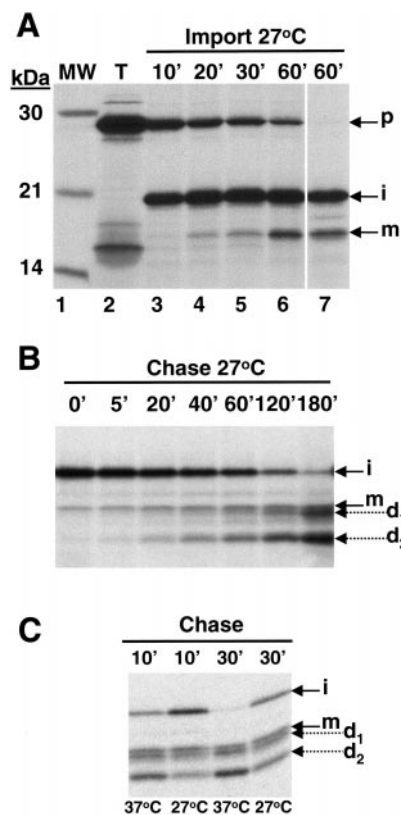
FIG. 5. **Import, two-step processing, and turnover rate of fxn in isolated rat liver mitochondria.** *A*, isolated rat liver mitochondria (20 mg/ml total protein) were incubated with radiolabeled p-fxn at 27 °C. At the indicated time points, 20-μl aliquots were removed and divided in two halves. Mitochondria from the first half were isolated by centrifugation and analyzed without further treatment (*lanes 3–6*). The second half was treated with 320 μg/ml proteinase K for 30 min at 0 °C followed by addition of 100 mM phenylmethylsulfonyl fluoride, after which the mitochondrial pellet was isolated by centrifugation, washed twice with 2 mM HEPES-KOH, pH 7.4, 220 mM D-mannitol, 70 mM sucrose, and 100 mM phenylmethylsulfonyl fluoride, and analyzed (shown only for the 60-min time point; *lane 7*). *B* and *C*, radiolabeled p-fxn was incubated with isolated rat liver mitochondria for 30 min at 27 °C. Proteinase K treatment was performed as described above, and the incubation was continued at 27 or 37 °C. Aliquots were withdrawn at the indicated time points and directly analyzed by SDS/PAGE.
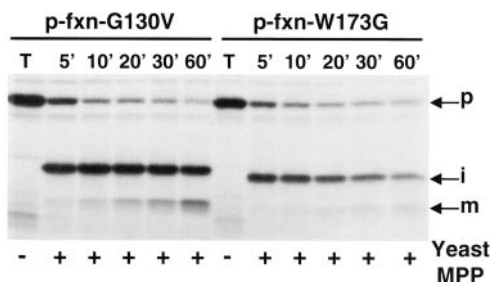
FIG. 6. **Two-step processing of mutant p-fxn-G130V and p-fxn-W173G by recombinant yeast MPP.** Experimental conditions were as described in the legend of Fig. 3*A*. T, control reactions incubated for 60 min without MPP.

mobility than the i and m products derived from wild type p-fxn (Fig. 7*A*), suggesting that the MPP cleavage sites might be different from those determined in Fig. 1 (*B* and *C*). The N terminus of i-fxn-G130V, however, was found to precisely correspond to that identified for wild type i-fxn (compare Fig. 7*B* and Fig. 1*B*). Thus, the observed effects of the G130V mutation (*i.e.* the reduced binding of p-fxn to MPP in a two-hybrid system (13) and the abnormal electrophoretic mobility of i-fxn-G130V and m-fxn-G130V on SDS/PAGE) have no bearing on precursor
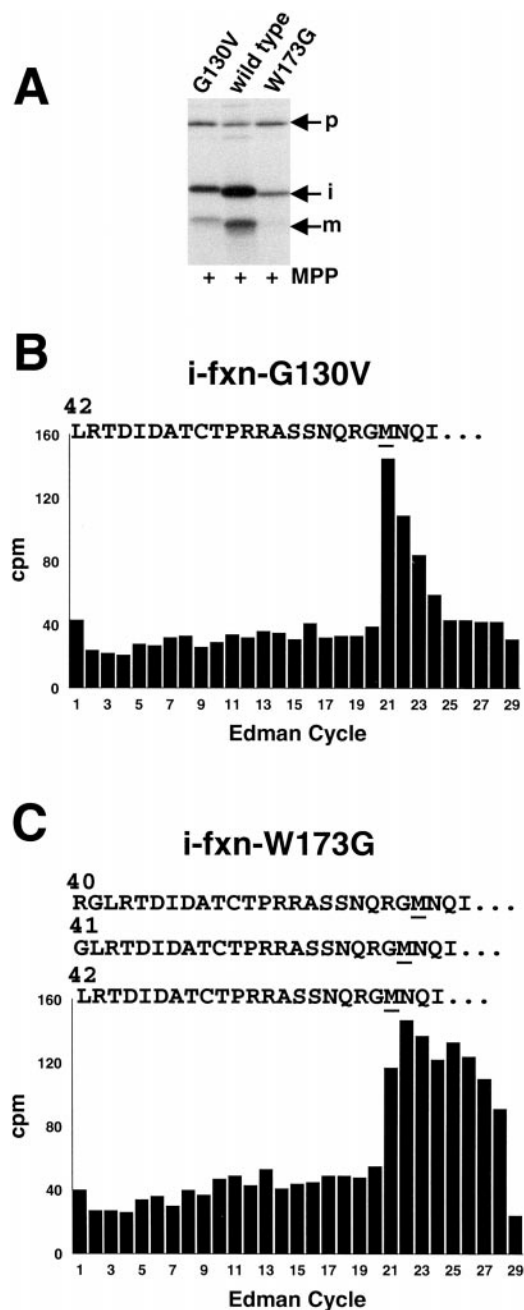

FIG. 7. **N-terminal radiosequencing of i-fxn-G130V and i-fxn-W173G.** *A*, two-step processing of p-fxn, p-fxn-G130V, and p-fxn-W173G precursors (denoted *wild type*, *G130V*, and *W173G*) as described in the legend to Fig. 3*A*, to show the abnormal electrophoretic mobility of the i and m products generated from p-fxn-G130V. *B* and *C*, N-terminal radiosequencing of i-fxn-G130V and i-fxn-W173G. Experimental conditions were as described in the legend of Fig. 1*B*.

processing.

The W173G FRDA Point Mutation Inhibits the i → m Processing Step—We also analyzed one additional mutation, W173G (8), and observed a rather different effect. Although the rate of p → i processing was normal, only a fraction of the i-fxn-W173G produced after 5 min of incubation with MPP was recovered after 60 min, and the m form was nearly undetectable (Fig. 6). This result was reproduced in independent processing reactions. When i-fxn-W173G was subjected to N-terminal radiosequencing, there was release of [35S]methionine in multiple successive cycles (Fig. 7*C*, cycles 21–25), consistent with a jagged N terminus and the presence of multiple sequences corresponding to N (Leu[42]), N+1, N+2, N+3, etc. This
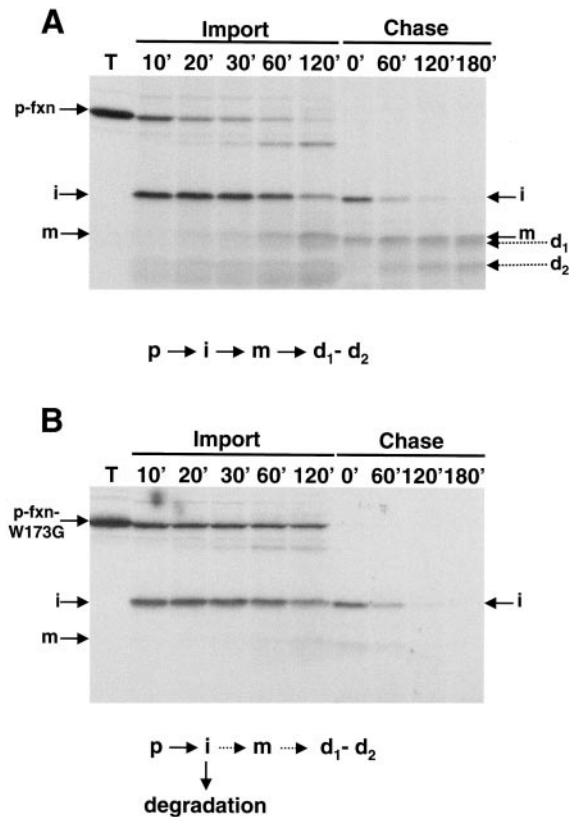
FIG. 8. **Import, two-step processing, and turnover rate of fxn-W173G in isolated rat liver mitochondria.** Import and chase reactions were performed as described in the legend of Fig. 5 (*A* and *B*, respectively). p-fxn (*A*) and p-fxn-W173G (*B*) were analyzed in parallel. The *schemes* at the bottoms of the panels show the two proposed proteolytic pathways.

result suggests that the W173G mutation affects the ability of MPP to cleave p-fxn at the correct site, generating abnormal intermediate molecules that cannot be processed to the mature form and are unstable. A similar effect could also arise from degradation by some bacterial protease in the MPP preparation, although this seems less likely given that we used a purified preparation of enzyme and that no such effect was observed with p-fxn and p-fxn-G130V under the same experimental conditions (Figs. 3*A* and 6).

Processing of p-fxn-W173G was also analyzed upon import into rat liver mitochondria. Here again, i-fxn-W173G was converted to only trace amounts of mature form, and during a 3-h chase, the accumulated i-fxn-W173G disappeared without any detectable production of m, d_1, or d_2 products (Fig. 8, compare *B* with *A*). This result is consistent with inhibition of the i → m step by the W173G mutation leading to instability of i-fxn-W173G. These data are in agreement with our recent finding that expression of a FRDA(W173G) cDNA in *yfh1Δ* cannot complement the lack of Yfh1p because of impaired processing and instability of i-fxn that lead to m-fxn deficiency and mitochondrial iron overload (19). Failure to observe the d_1 and d_2 products during import of p-fxn-W173G indicates that they normally originate from the mature form. The d_2 product was detected in *yfh1Δ*[pG3-FRDA] cells (Fig. 2*A*), whereas *yfh1Δ*[pG3-FRDAMet] cells, that express a C-terminally tagged version of p-fxn, showed a slightly larger d_2 product (not shown), indicating that d_2 represents a C-terminal fragment of p-fxn. Collectively, these results support a conserved proteolytic pathway, p → i → m → d_1 → d_2, that limits the levels of mature frataxin in mitochondria.

DISCUSSION

We have characterized two-step processing of human frataxin, fxn, by the general MPP. A substrate-product relationship between p-fxn and i-fxn and between i-fxn and m-fxn has been established. The two MPP cleavage sites have been identified, and m-fxn has been shown to correspond to endogenous frataxin in human tissues. Most mitochondrial protein precursors carry positively charged N-terminal presequences that are cleaved in a single step by MPP during or upon translocation to the mitochondrial matrix (16). Two-step processing by MPP is a rare variation that was first described for the *N. crassa* ATPase subunit 9 (17) and, more recently, yeast and human frataxin (Ref. 12 and this study). The targeting signals of these three proteins are 68, 51, and 55 residues long, 1.5–2 times the average mitochondrial presequence (20–40 residues) (26, 27), which may explain why they are removed in more than one cleavage. It has been proposed that a longer targeting signal is required by the ATPase subunit 9 to compensate for the hydrophobicity of the mature protein, which could otherwise affect solubility and import competence (17). By analogy, longer targeting signals may be required by yeast and human frataxin to neutralize the acidity of the mature protein, which may interfere with the initial steps of mitochondrial import (16). We are currently investigating this hypothesis by mutational analysis of the yeast frataxin precursor.

In analyzing the kinetics of two-step processing, we have found that MPP cleaves p-fxn at a much faster rate than i-fxn. The p → i reaction was 40 times faster than the i → m reaction with yeast MPP and 12 times faster with rat MPP. An excess of enzyme was used in all cases and most p-fxn was converted to i-fxn within the first 5 min of incubation, indicating that the lower rate of the i → m reaction did not depend on enzyme or substrate depletion. Previous surveys of known MPP cleavage sites have shown that the enzyme prefers an arginine residue at position −2 (25–27). Accordingly, both cleavage sites in the p-fxn presequence match the motif R*X* ↓ (*X*/S). Other studies, however, have shown that the residues around the cleavage site play a role in the context of the overall secondary structure of the presequence, which probably represents the most important determinant for substrate recognition by MPP (reviewed in Ref. 28). In the specific case of p-fxn, the first cleavage removes most of the presequence (residues 1–41), leaving only 14 residues at the protein N terminus to be removed by the second cleavage. The amino acid stretch removed by the second cleavage is therefore shorter than the average length of mitochondrial presequences, although presequences as short as 8 amino acids have been reported (27). In addition, these 14 residues have an helix content of 0.36%, lower than that of residues 1–41 (0.77%), as determined using an algorithm to predict the helical content of peptides (23). In the case of pYfh1p, the amino acid stretch removed by the second cleavage is more similar in length and helix content to the stretch removed by the first cleavage (residues 1–20, 1.21% helix; residues 21–51, 1% helix), and in fact, under our experimental conditions, the iYfh1p → mYfh1p step was as fast as the pYfh1p → iYfh1p step (not shown). These data suggest that the structure of the p-fxn presequence is responsible for the low rate at which i-fxn is processed to mature form. It is also possible that the first cleavage results in a conformational change that affects the ability of MPP to carry out the second cleavage. The rate of p → i processing was similar between rat and yeast MPP, whereas the rate of the i → m reaction decreased ~4 times with rat MPP and ~40 times with yeast MPP. This supports the idea that the second cleavage depends on structural determinants that may be species-specific. Given that the α and β subunits of rat MPP show 80–90% overall

sequence identity to the human MPP subunits (28), we have assumed that the rates at which rat MPP cleaves p-fxn and i-fxn are representative of the rates at which the human peptidase would cleave these substrates. However, we cannot exclude the possibility that the rate of i → m processing would be faster (or slower) in a fully homologous system.

The mature form, not the intermediate, is the predominant species detected in human tissues at steady state, suggesting that, under physiologic conditions, the number of precursor molecules that are imported and processed to i-fxn do not exceed the rate at which i-fxn is cleaved to the mature form. In isolated mitochondria, however, p-fxn was imported and processed to i-fxn in excess of the rate at which i-fxn could be cleaved to mature form, leading to i-fxn accumulation. Because over 50% of the input p-fxn was imported and processed to i-fxn even after substantial amounts of i-fxn had accumulated (Fig. 5*A*), the accumulation of i-fxn resulted not from saturation of the import machinery but rather from the different rates at which MPP cleaves p-fxn and i-fxn.

Whereas the i-fxn accumulated *in vitro* was eventually converted to an equal amount of mature form by rat MPP (Fig. 4*A*), additional proteolytic steps were observed within mitochondria (Fig. 5). Here, the accumulated i-fxn was quantitatively processed to two small C-terminal fragments without any significant changes in the levels of m-fxn. Failure to detect the C-terminal fragments when the i → m reaction was inhibited by the W173G mutation (Fig. 8*B*) indicates that these fragments most likely originate from cleavage of m-fxn. Therefore, we have proposed that p-fxn undergoes a p → i → m → d_1 → d_2 sequence of proteolytic reactions, with i → m representing the rate-limiting step. We have shown that MPP is responsible for the p → i and i → m steps; the enzyme responsible for the m → d_1 → d_2 steps remains to be identified. Because the rate of i → m did not exceed the rate of m → d_1 → d_2, the levels of m-fxn did not change during chases as long as 3 h. In contrast, i-fxn was progressively and almost quantitatively converted to d_2 (Fig. 5*B*). This suggests that the p → i → m → d_1 → d_2 pathway may limit the levels of frataxin present in mitochondria at any given time. In agreement with this view, we detected d_2 in the fxn-overexpressing *yfh1*Δ[pG3-FRDA] and *yfh1*Δ[pG3-FRDAMet] strains (Fig. 2*A* and not shown), but not in human tissues at steady state, a condition under which frataxin expression is probably carefully regulated.

One implication of our findings is that any factors that decrease the already low rate of i-fxn processing or accelerate m-fxn degradation could further reduce the steady state levels of frataxin. Whereas the G130V mutation did not have any obvious effect on two-step processing, the W173G mutation inhibited production of m-fxn, both *in vitro* and in isolated rat liver mitochondria. Moreover, we have recently shown that expression of the FRDA(W173G) allele in yeast cells lacking endogenous Yfh1p leads to m-fxn deficiency with a typical *yfh1*Δ phenotype (19). These results suggest that a processing defect may contribute to disease severity in FRDA patients with the W173G mutation (8), and in general, that point mutations in frataxin, or even MPP, may worsen frataxin deficiency in FRDA. Future studies will address the possibility to improve frataxin levels by stimulating processing of i-fxn by MPP or inhibiting the protease(s) responsible for degradation of m-fxn.

REFERENCES

1. Puccio, H., and Koenig, M. (2000) *Hum. Mol. Genet.* **9,** 887–892
2. Babcock, M., de Silva, D., Oaks, R., Davis-Kaplan, S., Jiralerspong, S., Montermini, L., Pandolfo, M., and Kaplan, J. (1997) *Science* **276,** 1709–1712
3. Foury, F., and Cazzalini, O. (1997) *FEBS Lett.* **411,** 373–377
4. Adamec, J., Rusnak, F., Owen, W. G., Naylor, S., Benson, L. M., Gacy, A. M., and Isaya, G. (2000) *Am. J. Hum. Genet.* **67,** 549–562
5. Harding, A. E. (1981) *Brain* **104,** 589–620
6. Campuzano, V., Montermini, L., Molto, M. D., Pianese, L., Cossee, M., Cavalcanti, F., Monros, E., Rodius, F., Duclos, F., Monticelli, A., and et al. (1996) *Science* **271,** 1423–1427
7. Campuzano, V., Montermini, L., Lutz, Y., Cova, L., Hindelang, C., Jiralerspong, S., Trottier, Y., Kish, S. J., Faucheux, B., Trouillas, P., Authier, F. J., Durr, A., Mandel, J. L., Vescovi, A., Pandolfo, M., and Koenig, M. (1997) *Hum. Mol. Genet.* **6,** 1771–1780
8. Cossee, M., Durr, A., Schmitt, M., Dahl, N., Trouillas, P., Allinson, P., Kostrzewa, M., Nivelon-Chevallier, A., Gustavson, K. H., Kohlschutter, A., Muller, U., Mandel, J. L., Brice, A., Koenig, M., Cavalcanti, F., Tammaro, A., De Michele, G., Filla, A., Cocozza, S., Labuda, M., Montermini, L., Poirier, J., and Pandolfo, M. (1999) *Ann. Neurol.* **45,** 200–206
9. Bradley, J. L., Blake, J. C., Chamberlain, S., Thomas, P. K., Cooper, J. M., and Schapira, A. H. (2000) *Hum. Mol. Genet.* **9,** 275–282
10. Cossee, M., Puccio, H., Gansmuller, A., Koutnikova, H., Dierich, A., LeMeur, M., Fischbeck, K., Dolle, P., and Koenig, M. (2000) *Hum. Mol. Genet.* **9,** 1219–1226
11. Knight, S. A., Sepuri, N. B., Pain, D., and Dancis, A. (1998) *J. Biol. Chem.* **273,** 18389–18393
12. Branda, S. S., Cavadini, P., Adamec, J., Kalousek, F., Taroni, F., and Isaya, G. (1999) *J. Biol. Chem.* **274,** 22763–22769
13. Koutnikova, H., Campuzano, V., and Koenig, M. (1998) *Hum. Mol. Genet.* **7,** 1485–1489
14. Gordon, D. M., Shi, Q., Dancis, A., and Pain, D. (1999) *Hum. Mol. Genet.* **8,** 2255–2262
15. Voisine, C., Schilke, B., Ohlson, M., Beinert, H., Marszalek, J., and Craig, E. A. (2000) *Mol. Cell. Biol.* **20,** 3677–3684
16. Neupert, W. (1997) *Annu. Rev. Biochem.* **66,** 863–917
17. Schmidt, B., Wachter, E., Sebald, W., and Neupert, W. (1984) *Eur. J. Biochem.* **144,** 581–588
18. Schena, M., Picard, D., Yamamoto, K. R. (1991) *Methods Enzymol.* **194,** 389–398
19. Cavadini, P., Gellera, C., Patel, P. I., and Isaya, G. (2000) *Hum. Mol. Genet.* **9,** 2523–2530
20. Branda, S. S., Yang, Z. Y., Chew, A., and Isaya, G. (1999) *Hum. Mol. Genet.* **8,** 1099–1110
21. Sikorski, R. S., and Boeke, J. D. (1991) *Methods Enzymol.* **194,** 302–318
22. Geli, V. (1993) *Proc. Natl. Acad. Sci. U. S. A.* **90,** 6247–6251
23. Villegas, V., Viguera, A. R., Aviles, F. X., and Serrano, L. (1996) *Fold. Des* **1,** 29–34
24. Matsudaira, P. (1987) *J. Biol. Chem.* **262,** 10035–10038
25. Gavel, Y., and von Heijne, G. (1990) *Protein Eng.* **4,** 33–37
26. Hendrick, J. P., Hodges, P. E., and Rosenberg, L. E. (1989) *Proc. Natl. Acad. Sci. U. S. A.* **86,** 4056–4060
27. Branda, S. S., and Isaya, G. (1995) *J. Biol. Chem.* **270,** 27366–27373
28. Fenton, W. A., and Kalousek, F. (1996) *Adv. Mol. Cell. Bio.* **17,** 163–191